CORONAVIRUS

SARS-CoV-2 viral clearance and evolution varies by type and severity of immunodeficiency

Yijia Li[1,2,3]†, Manish C. Choudhary[1]†, James Regan[1,4]†, Julie Boucau[5], Anusha Nathan[5,6], Tessa Speidel[7], May Yee Liew[2,8], Gregory E. Edelstein[1], Yumeko Kawano[1], Rockib Uddin[2,8], Rinki Deo[1], Caitlin Marino[5], Matthew A. Getz[5], Zahra Reynolds[2], Mamadou Barry[2], Rebecca F. Gilbert[2], Dessie Tien[2], Shruti Sagar[2], Tammy D. Vyas[2], James P. Flynn[1], Sarah P. Hammond[2], Lewis A. Novack[1], Bina Choi[1], Manuela Cernadas[1], Zachary S. Wallace[2], Jeffrey A. Sparks[1], Jatin M. Vyas[2,5], Michael S. Seaman[7], Gaurav D. Gaiha[2,5], Mark J. Siedner[2]*, Amy K. Barczak[2,5]*, Jacob E. Lemieux[2,8]*, Jonathan Z. Li[1]*

Despite vaccination and antiviral therapies, immunocompromised individuals are at risk for prolonged severe acute respiratory syndrome coronavirus 2 (SARS-CoV-2) infection, but the immune defects that predispose an individual to persistent coronavirus disease 2019 (COVID-19) remain incompletely understood. In this study, we performed detailed viro-immunologic analyses of a prospective cohort of participants with COVID-19. The median times to nasal viral RNA and culture clearance in individuals with severe immunosuppression due to hematologic malignancy or transplant (S-HT) were 72 and 40 days, respectively, both of which were significantly longer than clearance rates in individuals with severe immunosuppression due to autoimmunity or B cell deficiency (S-A), individuals with nonsevere immunodeficiency, and nonimmunocompromised groups ($P < 0.01$). Participants who were severely immunocompromised had greater SARS-CoV-2 evolution and a higher risk of developing resistance against therapeutic monoclonal antibodies. Both S-HT and S-A participants had diminished SARS-CoV-2–specific humoral responses, whereas only the S-HT group had reduced T cell–mediated responses. This highlights the varied risk of persistent COVID-19 across distinct immunosuppressive conditions and suggests that suppression of both B and T cell responses results in the highest contributing risk of persistent infection.

INTRODUCTION

Coronavirus disease 2019 (COVID-19) vaccinations have markedly transformed the landscape of the COVID-19 pandemic by offering substantial protection against infection acquisition and severe diseases (*1*, *2*) and have ultimately averted tens of millions of deaths (*3*). Unfortunately, not all individuals respond to vaccination equally well, and immunocompromised individuals can have poor vaccine responses (*4*, *5*) and worse COVID-19–related outcomes (*6*, *7*). Each new variant of severe acute respiratory syndrome coronavirus-2 (SARS-CoV-2) brings risks of resistance to current treatments, particularly targeted antibody therapies (*8*, *9*); resistance to vaccine-induced and naturally acquired immunity (*9*, *10*); and increased transmissibility (*10*). Immunocompromised individuals have been observed to harbor detectable SARS-CoV-2 virus for longer than nonimmunocompromised individuals (*11*–*13*). Such individuals represent a potential origin of novel SARS-CoV-2 variants, because persistent infection has been associated with accelerated viral evolution (*11*, *13*). However, the immunocompromised state is composed of a range of conditions and immune defects. Those defects that predispose an individual to persistent COVID-19 remain undercharacterized. Although there have been a number of case reports of persistent COVID-19 in immunosuppressed individuals (*11*–*16*) showing excessively prolonged viral shedding, persistent disease, and intrahost virological genetic diversity, there remains a need for larger-scale studies with a comprehensive virologic and immunologic characterization to better elucidate the immunologic risk factors for and mechanisms of persistent infection. To this end, we present here a detailed longitudinal virological and immunological analysis of a cohort of immunocompromised and nonimmunocompromised participants with SARS-CoV-2 infection with the goal of characterizing the virologic spectrum of persistent infection and exploring the immunologic determinants that predispose to its occurrence.

RESULTS

Participant characteristics

Fifty-six immunocompromised participants and 184 nonimmunocompromised participants enrolled in the Post-Vaccination Viral Characteristics Study (POSITIVES) longitudinal cohort study were included in this analysis (*17*–*19*). Demographic information and key viral characteristics are shown in Table 1. Immunocompromised participants were significantly older than nonimmunocompromised controls (median 55 versus 46 years, $P = 0.001$) and were more likely to receive monoclonal antibody (mAb) or antiviral treatment against SARS-CoV-2. The two groups had comparable sex, race, and ethnicity profiles and a similar median time from symptom onset or first positive COVID-19 test to enrollment (5 days versus 4 days). We further subdivided

[1]Department of Medicine, Brigham and Women's Hospital, Harvard Medical School, Boston, MA 02115, USA. [2]Department of Medicine, Massachusetts General Hospital, Harvard Medical School, Boston, MA 02114, USA. [3]University of Pittsburgh Medical Center, Pittsburgh, PA 15213, USA. [4]Department of Microbiology, Perelman School of Medicine, University of Pennsylvania, Philadelphia, PA 19104, USA. [5]Ragon Institute of MGH, MIT and Harvard, Cambridge, MA 02139, USA. [6]Program in Health Sciences and Technology, Harvard Medical School and Massachusetts Institute of Technology, Boston, MA 02115, USA. [7]Center for Virology and Vaccine Research, Beth Israel Deaconess Medical Center, Harvard Medical School, Boston, MA 02215, USA. [8]Broad Institute of MIT and Harvard, Cambridge, MA 02142, USA.
*Corresponding author. Email: msiedner@mgh.harvard.edu (M.J.S.); abarczak@mgh.harvard.edu (A.K.B.); jelemieux@partners.org (J.E.L.); jli@bwh.harvard.edu (J.Z.L.)
†These authors contributed equally to this work.

immunocompromised participants into the severe hematologic-oncology/transplant (S-HT, $n = 12$), severe autoimmune/B cell deficient (S-A, $n = 13$) and nonsevere (NS, $n = 31$) groups (refer to tables S1 and S2 for detailed categorization). Three participants died because of severe COVID-19 or COVID-19–related complications, all of whom were in the severe immunocompromised subgroups (S-HT, $n = 2$ and S-A, $n = 1$). Median follow-up duration for immunocompromised and nonimmunocompromised groups was 18 and 16.5 days ($P < 0.001$; Table 1). Eight participants in the nonimmunocompromised group had a follow-up duration of less than 10 days. Seventy-nine percent of immunocompromised and 88% of nonimmunocompromised participants cleared their nasal SARS-CoV-2 viral RNA at the end of the follow-up period. The median duration since the last vaccine was 154 days among 213 participants who were vaccinated, and relatively few participants (12%) had received Omicron-based boosters. One hundred and forty-seven participants agreed to provide blood samples; the median time to blood draw 1 (shortly after study entry) was 7 days after symptom onset or first positive polymerase chain reaction (PCR) test, and the median time to blood draw 2 was 20 days after symptom onset or first positive PCR test.

Delayed viral clearance was observed in participants in the S-HT cohort

We first aimed to characterize viral dynamics in the upper respiratory tract in participants with different categories of immunocompromising conditions. Immunocompromised and nonimmunocompromised participants had similar peak viral RNA loads (5.1, 5.1, 4.9, and 5.7 $\log_{10}$ SARS-CoV-2 copies/ml in S-HT, S-A, NS, and nonimmunocompromised groups; $P = 0.5$). However, the rates of nasal viral RNA decay were different between the immunocompromising categories, with

Table 1. Demographic and clinical information. Q1 and Q3, quartile 1 and quartile 3; AA, African American. Four participants received mAb after blood draws. Symptom duration indicates the duration between symptom onset (patient report or first positive test if asymptomatic screening) and first nasal swab collected by the study group. Variant information was obtained by either *S* gene or whole genome sequencing or by epidemiological information (time period when the participant was infected).

	Immunocompromised ($N = 56$)	Nonimmunocompromised ($N = 184$)	Total ($N = 240$)	*P* value
Sex, *n* (%)				0.2
Female	32 (57.1)	126 (68.5)	158 (65.8)	
Male	24 (42.9)	58 (31.5)	82 (34.2)	
Age, median (Q1, Q3)	55 (45, 67)	46 (33, 59)	49 (34, 60)	0.001
Race, *n* (%)				0.8
Asian	1 (1.8)	10 (5.4)	11 (4.6)	
Black or AA	5 (8.9)	19 (10.3)	24 (10.0)	
Other/unknown	5 (8.9)	16 (8.7)	21 (8.8)	
White	45 (80.4)	139 (75.5)	184 (76.7)	
Ethnicity				0.5
Hispanic or Latino	5 (8.9)	17 (9.2)	22 (9.2)	
Not Hispanic or Latino	47 (83.9)	143 (77.7)	190 (79.2)	
Other/unknown	4 (7.1)	24 (13.0)	28 (11.7)	
Inpatient, *n* (%)	7 (12.5)	8 (4.3)	15 (6.2)	0.051
Number of vaccinations, median number (Q1, Q3)	3 (3, 4)	3 (2, 3)	3 (2, 4)	<0.001
mAb use, *n* (%)	24 (42.9)	10 (5.4)	34 (14.2)	<0.001
Antiviral use, *n* (%)	39 (69.6)	57 (31.0)	97 (40.4)	<0.001
Immunocompromised group, *n* (%)				<0.001
S-HT	12 (21.4)	0 (0.0)	12 (5.0)	
S-A	13 (23.2)	0 (0.0)	13 (5.4)	
NS	31 (55.4)	0 (0.0)	31 (12.9)	
None	0 (0.0)	184 (100.0)	184 (76.7)	
Symptom duration, median days (Q1, Q3)	5 (4, 7)	4 (3, 6)	4 (3, 6)	0.04
Follow-up duration, median days (Q1, Q3)	18 (16, 30)	16.5 (15, 19)	17 (15, 20)	<0.001
Variant				<0.001
Delta	3 (5.4)	43 (23.4)	46 (19.2)	
Omicron	48 (85.7)	137 (74.5)	185 (77.1)	
Other/unknown	5 (8.9)	4 (2.2)	9 (3.8)	

the S-HT group demonstrating slower viral clearance compared with other groups (Fig. 1, A and B). Median time to nasal viral RNA clearance in the S-HT group was 72 days [95% confidence interval (CI): 5, not available (NA)] compared with 10 (7, NA) days for the S-A group, 12 (9, 17) days for the NS group and 13 (13, 15) days for the nonimmunocompromised group (log-rank, $P = 0.002$; Fig. 1B). Similarly, the S-HT group experienced a delay in the clearance of culturable virus (Fig. 1, C and D). Median time to viral culture clearance in the S-HT group was 40 days (95% CI: 5, NA) compared with 6.5 (5, NA) days for the S-A group, 6 days (5, 7) for the NS group, and 7 days (6, 7) for the nonimmunocompromised group (log-rank, $P < 0.001$; Fig. 1D). At or after 30 days from symptom onset or first positive test, 50, 15, and 6.5% of participants from S-HT, S-A, and NS groups had detectable viral RNA compared with 0% in the nonimmunocompromised group ($P < 0.0001$; fig. S1A). In addition, 50% of S-HT and 8.3% of S-A participants still had culturable virus compared with 0% in the NS and nonimmunocompromised groups after 30 days ($P < 0.0001$; fig. S1B). Viral dynamics for participants who did not clear viral RNA after 30 days (table S3) are shown in fig. S1C. Compared with the nonimmunocompromised group, the S-HT group was significantly associated with delayed viral RNA clearance [adjusted hazard ratio (aHR) for viral clearance of 0.29, 95% CI: 0.11 to 0.74, $P = 0.009$) and culturable virus clearance (aHR of 0.27 for viral clearance, 95% CI: 0.12 to 0.62, $P = 0.002$), after adjusting for demographics, number of vaccinations, and antiviral use (Table 2). To validate this finding, we also performed restricted mean survival time (RMST) analysis that does not require proportional hazard assumptions. Similarly, the S-HT group required significantly longer times to clear nasal SARS-CoV-2 viral RNA (adjusted RMST ratio of 3.09, 95% CI: 2.16 to 4.40, $P < 0.0001$) and culturable virus (adjusted RMST ratio of 3.33, 95% CI: 2.16 to 5.14, $P < 0.0001$) (Table 2).

Increased SARS-CoV-2 evolution and genetic diversity were observed in immunocompromised participants

We used a gene-specific next-generation sequencing approach to quantify the number of unique intrahost single-nucleotide variants

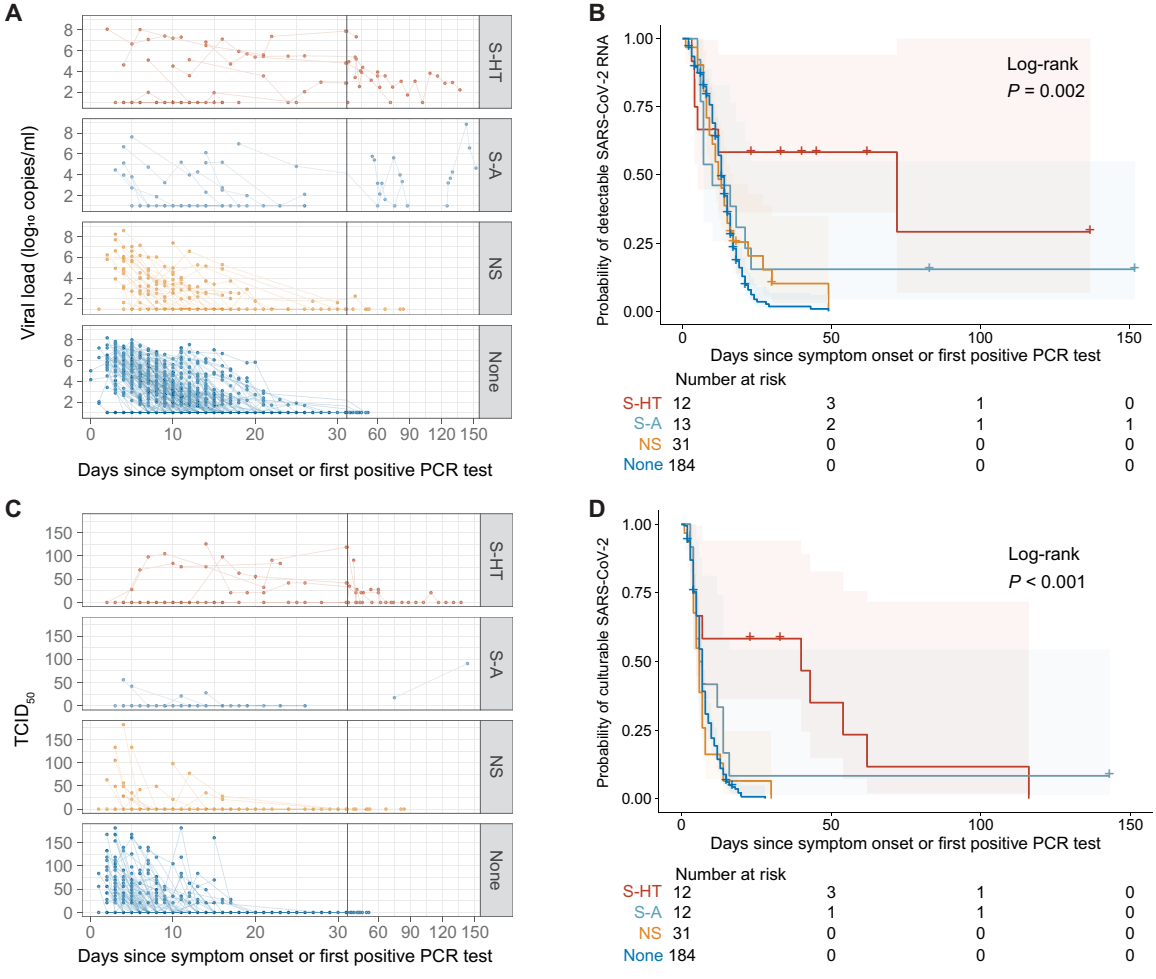

Fig. 1. Kinetics of SARS-CoV-2 viral RNA and culturable virus varied among the immunocompromised groups. (**A**) Upper respiratory viral RNA decay is shown. The lower level of quantification (LLOQ) is 10 copies/ml. (**B**) Kaplan-Meier estimates of upper respiratory viral clearance are shown (viral load below LLOQ), and global log-rank *P* values were shown. For (A) and (B), $n = 12$, 13, 31, and 184 for S-HT, S-A, NS, and nonimmunocompromised groups, respectively. (**C**) Upper respiratory culturable virus dynamics were quantified as $TCID_{50}$ values. (**D**) Kaplan-Meier estimates of upper respiratory culturable virus clearance were shown, and global log-rank *P* values were shown. For (C) and (D), $n = 12$, 12, 31, and 184 for S-HT, S-A, NS, and nonimmunocompromised groups, respectively.

Table 2. Association between immunocompromised groups and SARS-CoV-2 viral decay. Ref, reference; RR, RMST ratio; aRR, adjusted RMST ratio.

Hazard ratio for SARS-CoV-2 viral RNA clearance				
Group	**HR (95% CI)**	***P***	**aHR* (95% CI)**	***P***
None (ref)				
S-HT	0.22 (0.10–0.52)	0.0005	0.29 (0.11–0.74)	0.009
S-A	0.61 (0.32–1.16)	0.1	0.60 (0.27–1.34)	0.2
NS	0.85 (0.56–1.29)	0.4	0.88 (0.56–1.38)	0.6
RMST ratio for SARS-CoV-2 viral RNA clearance				
Group	RR	*P*	aRR* (95% CI)	*P*
Other groups (ref)				
S-HT	3.99 (2.14–7.47)	1.5×10^{-5}	3.09 (2.16–4.40)	5.3×10^{-10}
Hazard ratio for SARS-CoV-2 culturable virus clearance				
Group	HR (95% CI)	*P*	aHR* (95% CI)	*P*
None (ref)				
S-HT	0.23 (0.11–0.48)	8.7×10^{-5}	0.27 (0.12–0.62)	0.002
S-A	0.54 (0.28–1.03)	0.06	0.53 (0.26–1.10)	0.09
NS	1.12 (0.76–1.66)	0.6	1.32 (0.87–2.01)	0.2
RMST ratio for SARS-CoV-2 culturable virus clearance				
Group	RR	*P*	aRR* (95% CI)	*P*
Other groups (ref)				
S-HT	4.56 (2.54–8.18)	3.9×10^{-7}	3.33 (2.16–5.14)	5.5×10^{-8}

*Age, sex at birth, race, ethnicity, number of vaccinations, monoclonal antibody use, and antiviral use were adjusted for in the multivariate models.

(iSNVs) in the *S* gene, encoding the spike protein, present at >3% frequency of the total viral population within each sample. This analysis was limited to participants with a viral genome available both at baseline and at a minimum of one follow-up time point. Severely immunocompromised (S-HT and S-A) participants harbored a greater number of emergent iSNVs over time compared with NS and nonimmunocompromised group participants (Fig. 2A). To evaluate viral diversity, we calculated the average pairwise distance both at the nucleotide and at the amino acid level per day. Nucleotide average pairwise distance per day was significantly higher in the severe immunocompromised (S-HT and S-A) groups compared with either nonsevere ($P = 0.001$ using Dunn's test with Benjamini-Hochberg adjustment) or nonimmunocompromised groups ($P < 0.001$ using Dunn's test with Benjamini-Hochberg adjustment; Fig. 2B). Similar results were obtained when the average pairwise distances were calculated for amino acids (fig. S2A). Among participants with longitudinal sequences available, 39% of the participants in immunocompromised group versus 12% in the nonimmunocompromised group had evidence of viral nucleotide changes (Fisher's exact $P < 0.001$; Fig. 2C and fig. S2B). These nucleotide changes were distributed across the entire length of the *S* gene (fig. S2B).

Severely immunocompromised individuals had increased risk of resistance to anti–SARS-CoV-2 mAb therapy

Deep sequencing analysis of the *S* gene was carried out to evaluate the dynamics of mutation emergence in the presence of mAb treatment because earlier reports have shown evidence of mAb resistance emergence both in immunocompromised and nonimmunocompromised participants (*13, 20–29*). In total, 34 participants across different study groups received mAb therapy, 10 in S-HT, 9 in S-A, 5 in NS, and 10 in nonimmunocompromised groups (table S4). Of these, we were able to evaluate the risk of resistance emergence in a subset of participants for whom sequences were available at both baseline and at least one follow-up time point. Five of nine (56%) severely immunocompromised participants (S-HT and S-A) developed mAb-specific resistance mutations (Fig. 2, D and E). This was a significantly higher rate than that found in the nonsevere or nonimmunocompromised groups [0/11 (0%) combined, Fisher's exact, $P = 0.008$; Fig. 2D]. In addition, a longer infection duration was associated with increasing accumulation of mutations (fig. S2C).

Suboptimal humoral responses were elicited by infection in severely immunocompromised participants

We next characterized the antibody response in immunocompromised and nonimmunocompromised participants. In participants with available serum samples ($n = 94$), including those who had previously received mAbs, we found no difference in neutralizing antibody (nAb) titers between the different immunocompromised and nonimmunocompromised groups at early and later sampling time points, although this analysis may have been limited because of individuals who received anti–SARS-CoV-2 mAb infusion before sample collection (either therapeutic or pre-exposure prophylaxis) (Fig. 3, A and B). The nonimmunocompromised group exhibited an increase in anti-ancestral and anti-variant spike protein–specific nAb titers during follow-up, whereas we did not observe a significant increase in antibody titers in the immunocompromised groups (Fig. 3, A and B). However, after excluding individuals with exposure to mAb therapies, the nonsevere immunocompromised group demonstrated a moderate increase in spike protein–specific nAb titers, whereas the severe immunocompromised group showed no changes; the nonimmunocompromised group

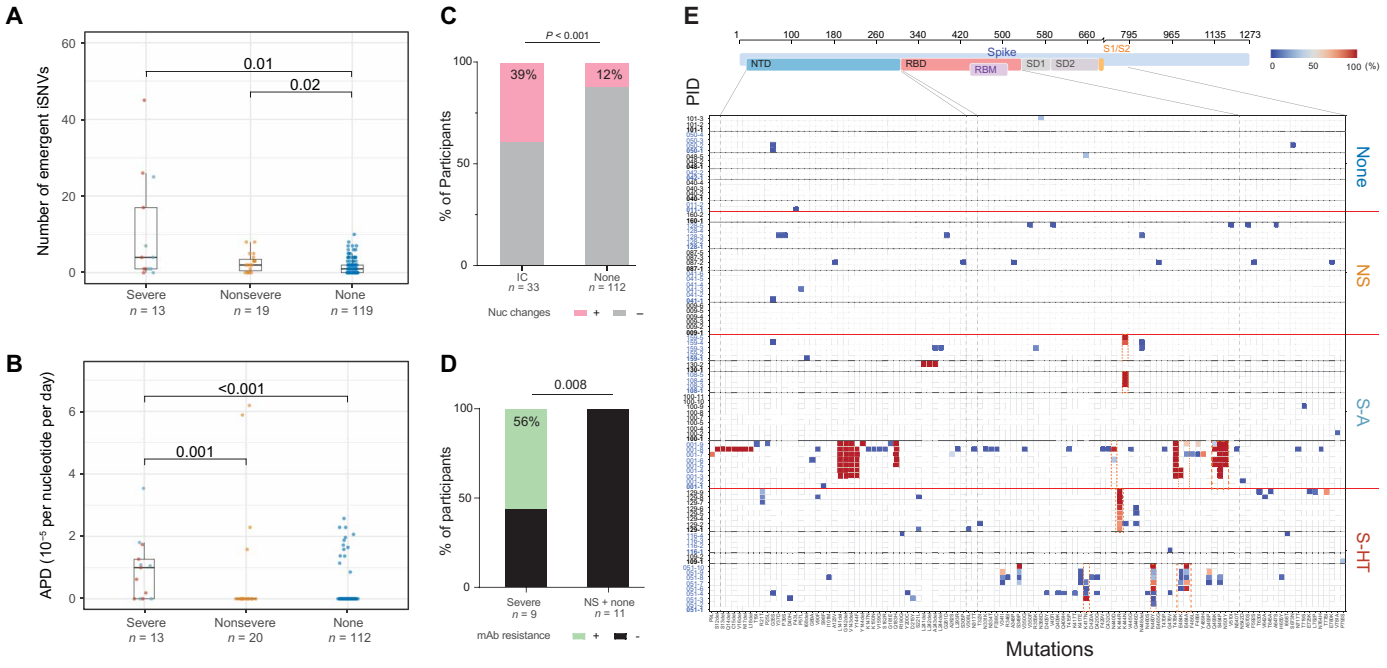

Fig. 2. SARS-CoV-2 intrahost mutations vary among different immunocompromised groups. (**A**) Numbers of iSNVs among severe (S-HT in red and S-A in green), nonsevere immunocompromised, and nonimmunocompromised (none) groups that emerged after the baseline time point are shown. (**B**) Nucleotide average pairwise distance (APD) are shown among the severe (S-HT in red and S-A in green), nonsevere immunocompromised (NS), and nonimmunocompromised (none) groups. (**C**) Percent of participants with any nucleotide changes during follow-up is shown. IC, immunocompromised. (**D**) Proportion of individuals with evidence of mAb resistance, categorized by those with severe or nonsevere/no immunosuppression, is shown. (**E**) Heatmap showing distribution of spike protein polymorphisms from participants receiving mAb treatment longitudinally. In the heatmap, the *y* axis indicates participants' IDs (PID) followed by sequential numbers of sample collection, and the *x* axis shows amino acid positions in the spike protein. Different domains of the spike protein are shown at the top. Colors indicate frequency of polymorphisms, with blue indicating the lowest value and red indicating the highest value on the scale. Participants in different study groups are separated by a red horizontal line. mAb resistance mutations are shown by red dotted boxes. Comparisons of iSNV and APD between groups in (A) and (B) were done using Dunn's test with Benjamini-Hochberg *P* value adjustment. Fisher's exact test was used in (C) and (D) to calculate significance between participants with and without viral evolution and in participants with and without mAb treatment–specific resistance mutations. Only significant *P* values are shown. NTD, N-terminal domain; RBD, receptor binding domain; RBM, receptor binding motif; S1, subunit 1; S2, subunit 2. Data in (A) and (B) are presented as Tukey's boxplots, with box indicating median and interquartile ranges and whiskers indicating 1.5× interquartile range.

demonstrated the greatest increase in nAb titers, plateauing between days 25 and 30 (Fig. 3, C and D).

In a multivariate generalized estimating equation (GEE) model, the anti-ancestral spike nAb titer in the severe group (S-HT and S-A) was approximately fivefold lower than in the nonimmunocompromised group (severe versus nonimmunocompromised, 0.18-fold, 95% CI: 0.05 to 0.60; fig. S3A). Similarly, the anti-variant spike nAb titer in the severe group was approximately 12-fold lower (severe versus nonimmunocompromised, 0.08-fold, 95% CI: 0.03 to 0.22; fig. S3B). Nonsevere immunocompromised status was not associated with differences in nAb changes as compared to the nonimmunocompromised group. In the whole cohort, each vaccine dose before SARS-CoV-2 infection was associated with 1.70-fold (95% CI: 1.25 to 2.30) and 1.35-fold (95% CI: 1.01 to 1.79) increase in anti-ancestral and anti-variant spike protein–specific antibody titers, respectively (fig. S3, A and B).

We also evaluated binding antibody titers against nucleocapsid protein because this assay is not affected by mAb use. Similar to the nAb data, individuals in the S-HT and S-A subgroups had blunted increases in nucleocapsid binding antibody (Ab) development from the acute time point to the later time point and lower binding Ab titers compared with the NS and nonimmunocompromised groups (Fig. 3E). Longitudinally, binding Ab titers in NS and nonimmunocompromised groups plateaued around days 20 to 25 at a concentration of 1 to 1.5 $\log_{10}$ IU/ml, whereas the S-HT and S-A groups exhibited delayed development of nucleocapsid binding Abs to a concentration below 1 $\log_{10}$ IU/ml after day 50 (Fig. 3F).

Diminished T cell responses to spike protein were observed in the S-HT group

In a recent study, Apostolidis *et al.* (*30*) demonstrated elevated spike protein–specific $CD8^+$ T cell responses in COVID-19 mRNA-vaccinated participants with multiple sclerosis receiving anti-CD20 treatment compared to healthy controls. Similarly, Zonozi *et al.* (*31*) noted similar findings of elevated interferon-γ (IFN-γ) secretion and $CD8^+$ T cell proliferation upon spike peptide pool stimulation in B cell–deficient individuals (either rituximab-treated or with common variable immune deficiency) compared with those without B cell deficiency. However, it remains largely unknown whether different types and degrees of immunosuppression are associated with a similar T cell immunophenotype after acute infection. To this end, we profiled the T cell effector function using an enzyme-linked immunosorbent spot (ELISpot) and an antigen-specific proliferation assay for a selected group of participants based on sample availability. The

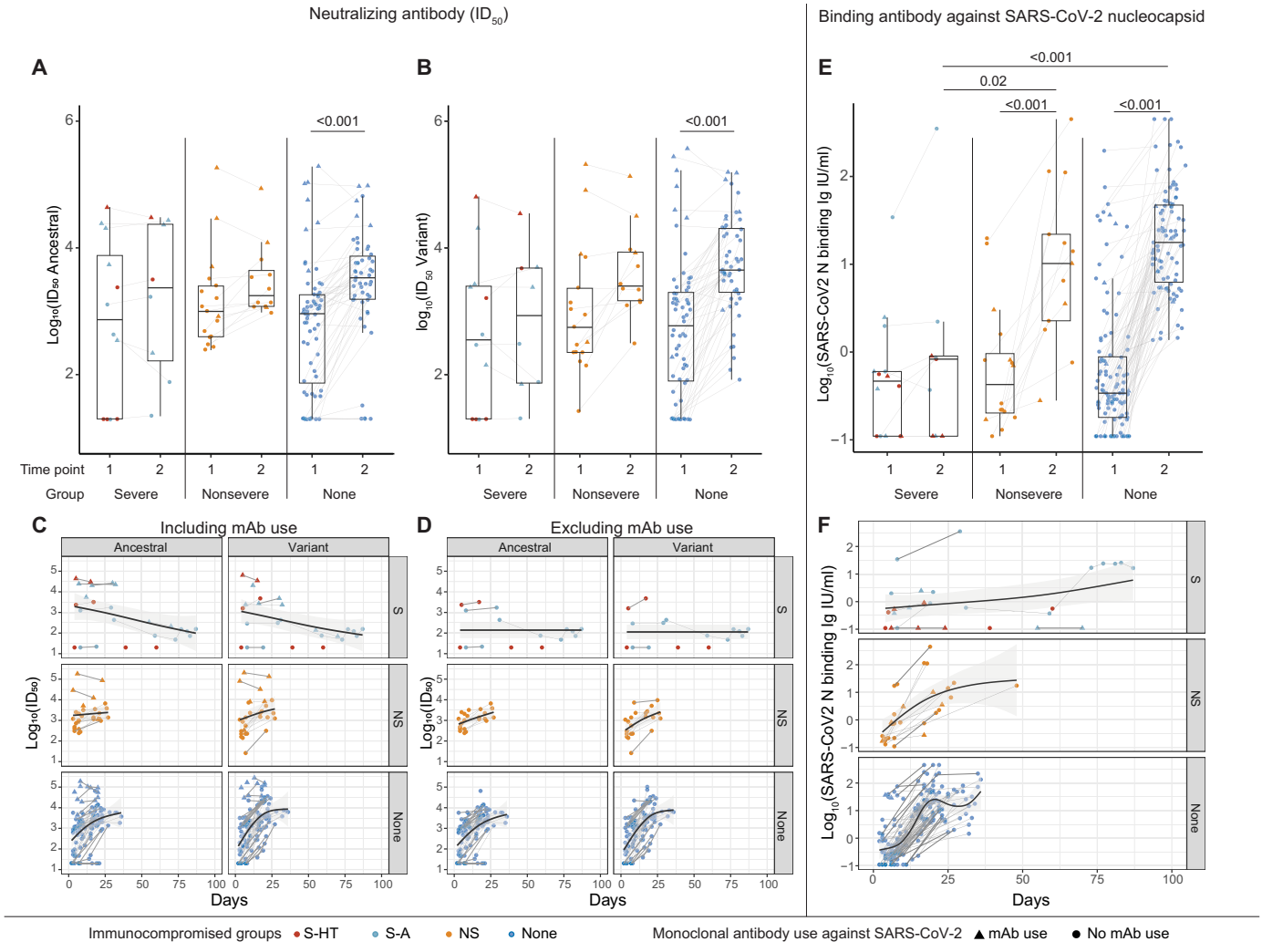

Fig. 3. Differences in nAb and nucleocapsid-binding Ab titers were observed among the different immunocompromised groups. (**A** and **B**) nAb titers were quantified as the ID_{50} against ancestral spike protein (A) and variant spike proteins (B). Variant-specific nAb titers were generated using a pseudoviral assay with the same spike protein variant (e.g., Delta, BA.1, BA.2, and BA.4/5) as that infecting the participant. (**C** and **D**) Longitudinal trajectories of nAb titers are shown for the different immunocompromised groups, including (C) or excluding (D) mAb use. For (A to C), $n = 5$, 7, 17, and 65 for S-HT, S-A, NS, and nonimmunocompromised groups, respectively. For (D), $n = 4$, 3, 13, and 57 in the S-HT, S-A, NS, and nonimmunocompromised groups after excluding mAb use. (**E**) Binding Ab titers against nucleocapsid protein were quantified for the indicated groups at the indicated time points. (**F**) Longitudinal trajectory of binding Ab titers is shown for the different immunocompromised groups. For (E) and (F), $n = 7$, 8, 18, and 111 for S-HT, S-A, NS, and nonimmunocompromised groups, respectively. Comparisons between different immunocompromised groups at the same time point in (A), (B), and (E) were performed using Dunn's test with Benjamini-Hochberg *P* value adjustment. Comparison of longitudinal Ab changes for participants with two blood draws were performed using the pairwise Wilcoxon rank sum test with Benjamini-Hochberg *P* value adjustment. Only significant *P* values are shown. Tukey boxplots were used to summarize Ab titers in (A), (B), and (E). A generalized additive model was used to evaluate the trend of Ab development in (C), (D), and (F), with 95% CIs in the shaded area. Lines between two time points indicate the same participants with two blood draws. The severe group included both S-HT and S-A, because they had comparable Ab titers at multiple time points.

nonimmunocompromised group had lower IFN-γ producing units per million cells upon stimulation at both blood draws (acute infection 0 to 14 days and post-acute 15 to 60 days after symptom onset or first positive COVID-19 test) compared with both NS and S-A groups in response to both ancestral and variant-specific spike peptide pools (Fig. 4A). Individuals in the S-A group tended to have the highest frequencies of proliferative $CD4^+$ and $CD8^+$ T cells upon spike peptide pool stimulation, especially compared with the S-HT and nonimmunocompromised individuals (Fig. 4, B and C, and fig. S4). In longitudinal analysis, the S-HT group showed poor $CD4^+$ and $CD8^+$ T cell proliferation despite comparable IFN-γ secretion as compared with the nonimmunocompromised group (Fig. 4D). In contrast, the S-A group showed robust T cell proliferation over time in response to both ancestral and variant-specific spike peptide pools compared to all other groups. We further performed a propensity score matched analysis to compare T cell responses around the time of study entry (time point 1) in participants with early versus delayed viral clearance (defined as clearance of SARS-CoV-2 viral RNA beyond day 30 or positive viral RNA beyond day 10 and then lost to follow-up) in the immunocompromised groups. In six participants with delayed viral

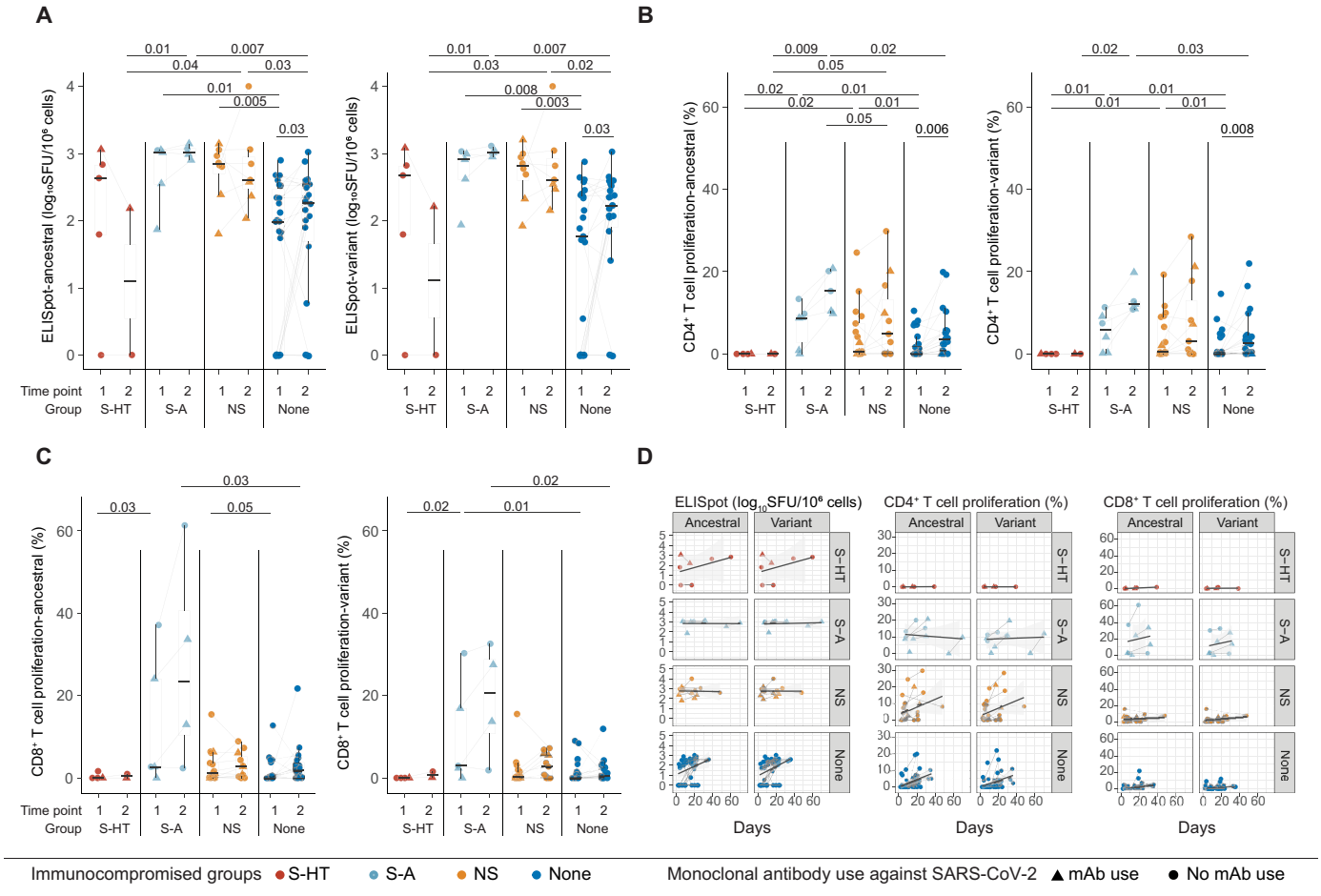

Fig. 4. Spike protein–specific T frequencies varied among different immunocompromised groups. (**A**) ELISpot assays were performed using peptide pools derived from ancestral and variant-specific spike protein. $N = 5$, 5, 8, and 26 for S-HT, S-A, NS, and nonimmunocompromised groups, respectively. (**B** and **C**) Frequencies of proliferating $CD4^+$ T cells (B) and $CD8^+$ T cells (C) were quantified in samples that were stimulated with ancestral or and variant spike peptide pools. For (B), $n = 4$, 6, 17, and 30 for S-HT, S-A, NS, and nonimmunocompromised groups, respectively. For (C), $n = 4$, 5, 17, and 30 for S-HT, S-A, NS, and nonimmunocompromised groups, respectively. (**D**) Longitudinal trajectories of spike protein-specific T frequencies in the indicated groups as measured by ELISpot (left) or proliferation assay (middle and right) are shown. Comparisons between different immunocompromised groups at the same time point were performed using Dunn's test with Benjamini-Hochberg *P* value adjustment. Comparison of longitudinal Ab changes for participants with two blood draws was performed using the pairwise Wilcoxon rank sum test with Benjamini-Hochberg *P* value adjustment. Only significant *P* values are shown. Tukey boxplots were used to summarize T cell responses for (A) to (C). A generalized additive model was used to evaluate the trend of T cell responses with 95% CIs in the shade area. Lines between two time points indicate the same participants with two blood draws.

clearance matched to 18 participants with early clearance (fig. S5A) based on binding Ab titers and severity of immunocompromise, we observed comparable binding Ab titers at study entry ($P = 0.3$; fig. S5B). ELISpot response was comparable between early and delayed groups (fig. S5, C and D). However, $CD4^+$ and $CD8^+$ T cell proliferation was higher in the early clearance group at study entry ($P < 0.05$ except panel H; fig. S5, E to H). We were unable to evaluate differences between groups at the second blood draw time point because of limited numbers.

DISCUSSION

Understanding viral and immune control characteristics of COVID-19 infection is crucial to our ability to care for immunocompromised individuals at the greatest risk of persistent and severe infection. Moreover, it can guide public health interventions and shed light on vaccine development that protects immunocompromised individuals. In this study, we performed an in-depth virologic and immunologic evaluation of a cohort of immunocompromised and nonimmunocompromised individuals. We demonstrated a hierarchy of immunocompromised conditions that increase the risk of delayed viral clearance and SARS-CoV-2 evolution, especially in those where both B and T cell responses are suppressed. Specifically, we found that individuals with a history of hematological malignancy and organ transplant demonstrated the greatest delay in viral clearance that may be mediated by suppression of both B and T cell responses. In contrast, those with B cell immunodeficiency had an intermediate risk of chronic infection in the setting of an immune response, showing the likely protective effect of a heightened SARS-CoV-2–specific T cell function.

Our cohort study confirmed findings from prior case reports and case series. In a review by Dioverti *et al.* (*32*), the authors summarized cases of persistent COVID-19 lasting from approximately 1 month to

1 year. These included a spectrum of immunocompromised hosts from individuals with solid organ transplants, hematological malignancy (*14, 20, 22, 23, 25, 29, 33–37*), and autoimmune diseases receiving immunosuppressive therapies. However, immunocompromise is a broad spectrum, and it has not been clear which immunosuppressive conditions represent the greatest risk for persistent infection. The results of our study provide critical insight as to the hierarchy of risk for delayed SARS-CoV-2 RNA and culture clearance, as well as viral evolution. Specifically, we found that individuals with solid organ transplant and hematological malignancy are associated with the longest period of viral RNA and culturable viral shedding, followed by severely immunocompromised participants with autoimmune conditions receiving B cell–depleting therapy and those with primary B cell deficiency. Participants with mild nonsevere immunocompromise, such as those with autoimmune diseases receiving antitumor necrosis factor treatment, had similar viral shedding dynamics to nonimmunocompromised participants.

There have been several prior case reports of immunosuppressed individuals with chronic COVID-19 and accumulation of viral polymorphisms and drug resistance mutations (*13, 14, 21, 27, 35*), but there has been little in the way of more systematic evaluation of viral evolution. In this study, we used *S* gene–specific deep sequencing to assess longitudinal viral evolution and diversity. Our results show that severe immunosuppression is associated with increased viral evolution and diversification. In addition, severely immunocompromised hosts had a greater risk of developing treatment-emergent resistance mutations to mAb therapy when compared with nonimmunocompromised participants. These findings highlight the potential for immunocompromised individuals to serve as a source for SARS-CoV-2 evolution and drug resistance, consistent with isolated reports of immunocompromised hosts implicated in the emergence of highly mutated SARS-CoV-2 variants (*13, 15, 16, 24, 28, 38–41*). It should be noted that, even within the category of severe immunocompromise, participants demonstrated a range of viral diversification and evolution patterns, and additional studies are needed to fully assess the drivers of accelerated viral evolution.

Another highlight of our study is our use of in-depth analysis of B and T cell responses, including SARS-CoV-2–specific neutralizing and binding Ab titers, as well as ELISpot and T cell proliferation studies. We noted lower titers of nAb against both ancestral virus and variant virus in the severe immunocompromised group (less than 10 to 20% compared with nonimmunocompromised individuals) after adjusting for vaccination doses, mAb use, and demographic confounders. Each additional dose of vaccination is associated with an approximately 1.5-fold increase in Ab titers in the whole cohort, underscoring the importance of adherence to COVID-19 vaccination recommendations. However, there is evidence that non–B cell immunity may be sufficient for the clearance of SARS-CoV-2. Early in the pandemic, cases were reported of individuals with X-linked agammaglobulinemia who developed COVID-19 pneumonia but subsequently recovered despite a lack of SARS-CoV-2–specific immunoglobulins or effective antiviral therapy (*42*). In our study, the risk of chronic infection was highest in S-HT participants. This group of participants was found to have both suboptimal humoral and cell-mediated immune responses. The "near-normal" frequencies of effector ELISpot responses in S-HT individuals, compared to the nonimmunocompromised group, is likely the result of exposure to high amounts of SARS-CoV-2 antigen, whereas the reduced proliferation demonstrates compromised functionality. In contrast, the S-A participants had even more robust SARS-CoV-2–specific proliferative T cell responses than the nonimmunocompromised group, indicating increased functional SARS-CoV-2–specific $CD8^+$ T cell responses, which was associated with an intermediate risk of chronic infection. When categorizing participants based on timing of viral clearance, even with comparable endogenous humoral response (measured by N binding Ab titers in this case), T cell proliferation response was different at the early stage of breakthrough infection (within 2 weeks) between those who had early versus delayed viral RNA clearance. These results align with some intriguing reports that individuals receiving anti-CD20 treatment may demonstrate stronger T cell responses, particularly more robust activation-induced marker-positive $CD8^+$ T cell responses (*30*), effector T cell response, and $CD8^+$ T cell proliferative capacity (*31*). We found that both $CD8^+$ T cell response and $CD4^+$ T cell responses, including proliferation in response to both ancestral and variant-specific spike peptides, were more pronounced in the S-A group compared with other nonimmunocompromised groups. Together with the results from other cohorts, our results raise the question of whether individuals with B cell deficiencies may have a lower risk of persistent SARS-CoV-2 infection due to preserved T cell function, either as a compensatory mechanism or T cell priming by certain B cell–depleting therapies.

There are several limitations to this study. We included a relatively small number of individuals with malignant hematological conditions or transplant history, and we were able to obtain blood samples from only a subset of the participants to characterize their humoral and T cell immunity. Larger studies are needed to provide greater precision as to the extent of immune defect or immunosuppressive medication that may place patients at the greatest risk of chronic infection and viral evolution. Immunocompromised groups had slightly longer follow-up duration than nonimmunocompromised group, but both groups were largely followed until their viral swabs were negative for quantifiable SARS-CoV-2 RNA or until they were lost to follow up. Nonimmunosuppressed individuals were more likely to be infected with the Delta variant, although we have previously shown no difference in viral decay rates between the Delta and Omicron variants (*17*). We also did not analyze markers reflecting innate immunity, including soluble inflammatory markers and monocyte phenotypes. Our study focused on virologic and immunologic responses after COVID-19, and it is unclear how these may contribute to persistence and severity of symptoms. Furthermore, we only evaluated spike protein-specific humoral and cellular immunity, although immunity targeting other structural or nonstructural proteins has been shown to alter disease course (*43, 44*). We observed that in the setting of suppressed B cell activity, the S-A group participants had the highest proliferation of SARS-CoV-2–specific T cells among all participant categories. This finding is consistent with recent reports of enhanced SARS-CoV-2–specific T cell responses in those receiving anti-CD20 agents and either SARS-CoV-2 vaccination or infection (*30, 31*). However, further mechanistic studies are needed to confirm that this is truly a compensatory effect in the absence of humoral immunity.

In conclusion, in this prospective cohort of well-characterized individuals with acute COVID-19, we demonstrated a correlation between a hierarchy of immunocompromised conditions and SARS-CoV-2 viral shedding, viral evolution, and adaptive immunity. Our results highlight the finding that the risk of chronic SARS-CoV-2 infection is not uniform across immunosuppressive conditions and provide clarity on which immunosuppression conditions predispose individuals to delayed SARS-CoV-2 RNA and culture clearance as

well as viral evolution. The high-risk populations identified in this study may benefit from targeted public health and additional therapeutic interventions. In addition, the results provide further insights on the humoral and cell-mediated immune correlates of viral clearance, which is crucial for the development of improved vaccines and future therapies.

MATERIALS AND METHODS

Study design

This study is a prospective cohort study enrolling consecutive participants with newly diagnosed COVID-19 (randomization and blinding not applicable). We did not specifically calculate the sample size and included the first 1000 participants screened in this cohort. This was done to ensure there were sufficient immunocompromised participants included in this current analysis. The overall objective of this prospective cohort study is to longitudinally evaluate the virological and immunological aspects of COVID-19 in a largely vaccinated population. This study did not provide additional treatment to the participants. Antivirals and mAb treatments were provided by participants' providers. Nasal swab viral load, viral culture, serological testing, and cellular immunity were measured longitudinally.

We enrolled participants with a positive COVID-19 test in the Mass General Brigham Medical HealthCare System as part of the POSITIVES (*17, 19*) in addition to one immunocompromised participant from our previous study (*13*). Each participant's medical record was reviewed for demographic data, immunosuppression status, and COVID-19 treatment history by board-certified clinicians. For the POSITIVES study, participants self-collected anterior nasal swabs every 2 to 3 days for a total of five to six samples over 2 weeks. All participants in the POSITIVES were offered the opportunity to collect additional swabs when possible and were followed until they had two consecutive negative PCR tests. For the one immunocompromised participant reported previously, nasopharyngeal swabs were collected by healthcare providers (*13*). In a subset of participants who agreed to provide blood samples, the first blood draw was done generally before day 15 of symptom onset (acute phase) or first positive PCR or antigen test for COVID-19, and the second blood draw was between 15 and 60 days after (post-acute phase) (fig. S6). This study was approved by Mass General Brigham Institutional Review Board (approval number: 2021P000812), and all participants have signed informed consent upon entry to the study.

Categorization for immunocompromised conditions

Immunocompromised participants were further categorized into the following groups: severe immunocompromised participants, which were further categorized into severe-hematological malignancy/transplant patients (S-HT), severe autoimmune patients (S-A; participants with autoimmune condition receiving B cell targeting agents or B cell deficiency), and nonsevere immunocompromised participants (NS). This categorization was based on a recent cohort study that demonstrated a hierarchy of Ab response to COVID-19 vaccinations in different medical conditions (*4, 45*). Detailed classification criteria are listed in table S1.

SARS-CoV-2 viral load assay

SARS-CoV-2 viral RNA was quantified as described previously (*46*). Briefly, virions were pelleted from nasal swab fluid by centrifugation at 21,000*g* for 2 hours at 4°C. TRIzol-LS Reagent (Thermo Fisher Scientific) was added to the pellet, vortexed, and incubated on ice for 10 min. Chloroform was added, and the solution was vortexed before centrifugation at 21,000*g* for 15 min at 4°C. RNA was isolated from the aqueous layer by isopropanol precipitation and eluted in diethyl pyrocarbonate–treated water (Thermo Fisher Scientific). SARS-CoV-2 RNA copies were quantified with an in-house viral load assay using the CDC 2019-nCoV_N1 primer and probe set (Integrated DNA Technologies). The efficiency of the RNA extraction and reverse transcription quantitative PCR (RT-qPCR) amplification was evaluated by quantifying the replication-competent avian sarcoma leukosis virus long terminal repeat with a splice acceptor (RCAS) RNA recovered from each sample and the two N1 controls. The importin-8 (*IPO8*) human housekeeping gene was also amplified and evaluated as a measure of sample collection quality. Samples were run in triplicate wells for N1 and in duplicate wells for RCAS and *IPO8*.

SARS-CoV-2 viral culture assay

Viral culture was performed as previously reported (*17*). Vero-E6 cells [the American Type Culture Collection (ATCC)] maintained in Dulbecco's modified Eagle's medium (DMEM; Corning) supplemented with Hepes (Corning), 1× penicillin (100 IU/ml)/streptomycin (100 μg/ml) (Corning), 1× glutamine (GlutaMAX, Thermo Fisher Scientific), and 10% fetal bovine serum (FBS; MilliporeSigma) were plated 16 to 20 hours before infection. Each sample consisting of nasal swab fluid was thawed on ice and filtered through a Spin-X 0.45-μm filter (Corning) at 10,000*g* for 5 min. Before infection, the medium was changed to DMEM supplemented with Hepes, 1× antibiotic/antimycotic (Thermo Fisher Scientific), 1× glutamine, 2% FBS, and polybrene (5 μg/ml; Santa Cruz Biotechnologies). Each filtered sample was then used to inoculate Vero-E6 cells by spinfection (2000*g* for 1 hour at 37°C). Each condition was plated in quadruplicate wells in 1:5 dilutions across half the plate. The plates were observed at 7 days after infection using a light microscope to check for cytopathogenic effect (CPE), and a median tissue culture infectious dose ($TCID_{50}$) was calculated for each sample.

Definitions for SARS-CoV-2 viral RNA clearance and culturable virus clearance

SARS-CoV-2 viral RNA clearance was defined as SARS-CoV-2 viral RNA from nasal swabs reached below the lower quantifiable (<10 copies/ml) threshold, and the viral RNA load was input as 10 copies/ml for statistical purposes. In participants who had viral rebound after initial viral clearance, we used the time point when viral RNA first became unquantifiable as long as the rebound viral RNA load was below 1000 copies/ml. We chose this threshold because it is consistent with previous viral rebound case definitions (*47*). For those who rebounded above 1000 copies/ml, we designated the next time point that viral RNA reached below 10 copies/ml as time for viral RNA clearance. For culturable virus clearance, we chose the first time point when there was no CPE effect, and where all subsequent samples did not have culturable viruses (if there were subsequent samples collected).

Neutralizing Ab responses and nucleocapsid binding Ab assay

Neutralizing activity against SARS-CoV-2 pseudovirus was measured using a single-round infection assay in 293T target cells expressing angiotensin converting enzyme 2 (ACE2) (293T/ACE2 target cells)

(*18*). Pseudotyped virus particles were produced in 293T/17 cells (ATCC) by cotransfection of plasmids encoding codon-optimized full-length spike protein (ancestral D614G, Delta, Omicron BA.1, Omicron BA.2, and Omicron BA.4/5), packaging plasmid pCMV ΔR8.2, and luciferase reporter plasmid pHR′ CMV-Luc. Packaging and luciferase plasmids were provided by B. Graham [National Institutes of Health (NIH); Vaccine Research Center]. The 293T cell line stably overexpressing the human ACE2 cell surface receptor protein was provided by M. Farzan and H. Ma (the Scripps Research Institute). For neutralization assays, serial dilutions of patient serum samples were performed in duplicate followed by addition of pseudovirus. Pooled serum samples from convalescent COVID-19 patients or prepandemic normal healthy serum were used as positive and negative controls, respectively. Plates were incubated for 1 hour at 37°C followed by addition of 293/ACE2 target cells (1×10^4 per well). Wells containing cells and pseudovirus (without sample) or cells alone acted as positive and negative infection controls, respectively. Assays were harvested on day 3 using Promega BrightGlo luciferase reagent, and luminescence was detected with a Promega GloMax luminometer (Promega). Titers are reported as the dilution of serum that inhibited 50% virus infection (ID_{50} titer). Pseudovirus-based neutralization assays were conducted using ancestral spike protein, as well as Delta and Omicron (BA.1, BA.2, or BA.4/5) spike protein. Anti-variant nAb titers were determined on the basis of the viral strain each participant was infected with (either by sequencing or in small proportion, imputed by time of infection when specific strain was prevalent). Binding Ab activity against nucleocapsid protein was measured using Coronavirus Ig Total Human 11-Plex ProcartaPlex Panel (Thermo Fisher Scientific) according to the manufacturer's instruction.

T cell ELISpot assay

The IFN-γ ELISpot assay used here was reported in our previous study and were performed according to the manufacturer's instructions (Mabtech) (*48*). Briefly, peripheral blood mononuclear cells (PBMCs) were incubated with SARS-CoV-2 peptide pools (MGH Peptide Core) at a final concentration of 0.5 μg/ml for 16 to 18 hours (100,000 to 200,000 cells per test). Anti-CD3 (0.5 μg/ml; clone OKT3, BioLegend) and anti-CD28 Ab (0.5 μg/ml; clone CD28.2, BioLegend) were used as positive controls. To quantify antigen-specific responses, mean spots of the dimethyl sulfoxide (DMSO) negative control wells were subtracted from the positive wells. The results were expressed as spot-forming units (SFU) per 10^6 PBMCs. Responses were considered positive if the results were >5 SFU/10^6 PBMCs after control subtraction. If negative DMSO control wells had >30 SFU/10^6 PBMCs or if positive control wells (anti-CD3/anti-CD28 stimulation) did not have >1000 SFU, the results were deemed invalid and excluded from further analysis.

T cell proliferation assay

T cell proliferation assay was reported previously (*48*). Briefly, PBMCs were incubated in phosphate-buffered saline with 0.5 μM carboxyfluorescein succinimidyl ester (CFSE; Life Technologies) or CellTrace Far Red (CTFR, Invitrogen) at 37°C for 20 min. Then, they were washed and resuspended at 0.5 to 1×10^6/ml and plated into 96-well U-bottom plates (Corning) in 200 μl of media. Peptide pools were added at a final concentration of 0.5 μg/ml, followed by incubation at 37°C with 5% CO_2 for 6 days. The PBMC staining Ab panels included the following: anti-CD3 phycoerythrin (PE)–cyanine (Cy) 7 (1:100 dilution; clone SK7; BioLegend; RRID: AB_10640737), anti-CD8 allophycocyanin (APC) (1:100 dilution; clone SK1; BioLegend; RRID: AB_2075388), anti-CD4 brilliant violet (BV) 711 (1:100 dilution; clone RPA-T4; BioLegend; RRID: AB_2564393), and LIVE/DEAD violet viability dye (Life Technologies). For PBMCs stained with CTFR proliferation dye (CTFR, Invitrogen), cells were then washed and stained with anti-CD3 APC-Cy7 (1:100 dilution; clone UCHT1; BioLegend; RRID: AB_830755), anti-CD8 BV605 (1:100 dilution; clone SK1; BioLegend; RRID: AB_2566513), anti-CD4 PE-Cy7 (1:100 dilution; clone OKT4; BioLegend; RRID: AB_571959), and LIVE/DEAD violet viability dye (Life Technologies). Cells were washed and fixed in 2% paraformaldehyde before flow cytometric analysis on a BD LSR II (BD Biosciences). A positive proliferation response was defined as a percentage of $CD3^+CD4^+$ or $CD3^+CD8^+$ $CFSE^{low}$ or $CTFR^{low}$ cells with at least 1.5× greater than the highest of two negative-control wells and greater than 0.2% $CFSE^{low}$ or $CTFR^{low}$ cells in magnitude after background subtraction.

SARS-CoV-2 *S* gene, whole-genome sequencing, and variant determination

SARS-CoV-2 viral RNA isolation was performed as described previously (*46*). RNA was converted to cDNA using SuperScript IV reverse transcriptase (Invitrogen) as per the manufacturer's instructions. *S* gene amplification was performed using a nested PCR strategy with in-house designed primer sets targeting codons 1 to 814 of the *S* gene as previously described (*28*). PCR products from different individuals were pooled, and Illumina library construction was performed using the Nextera XT Library Prep Kit (Illumina). Sequencing was performed on the Illumina MiSeq platform, and deep sequencing data analysis was carried out using the Stanford Coronavirus Antiviral & Resistance Database (CoVDB) platform (https://covdb.stanford.edu/sierra/sars2/by-reads/?cutoff=0.01&mixrate=0.01) (*49*). Input FASTQ sequence alignment with Wuhan-Hu-1 reference was done using MiniMap2 version 2.22 in CodFreq pipeline (https://github.com/hivdb/codfreq). The output of MiniMap2, an aligned SAM file, was converted to a CodFreq file by a publicly available pipeline using a PySam library (version 0.18.0) and further analyzed with the CoVDB (*49, 50*). PCR and sequencing runs were performed once with the appropriate positive and negative controls. For *S* gene analysis, amino acid variants were called at the codon level using perl code and used for resistance interpretation with a 1% limit of detection. The accuracy of the deep sequencing platforms was evaluated with a control library of clonal SARS-CoV-2 sequences mixed at known concentrations as described previously (*51*). Mutations detected by next-generation sequencing at below 20% of the viral population were labelled as "low-frequency" variants because they would largely be missed by traditional Sanger sequencing. A minimum average of 500× sequencing coverage per sample was required for variant calling. SARS-CoV-2 variant calling was done using three different variant calling platforms, namely, CoVDB (*49*), Scorpio call version v1.2.123 (https://pangolin.cog-uk.io/), and Nextclade version 1.13.2 (https://clades.nextstrain.org/) (*52*). Next-generation sequencing data used for data analysis in this manuscript are available on the National Center for Biotechnology Information Sequence Read Archive (SRA) with accession number PRJNA1027562. SARS-CoV-2 WGS was performed on the basis of the protocol described in our previous publications (*17, 19*). Variant information was obtained by *S* gene sequencing (described above), whole-genome sequencing (WGS) (*17*), or epidemiological information (time period when the participant was infected if *S* gene sequencing or WGS information was not available).

SNV, genetic diversity analysis, and mAb resistance mutation analysis

For assessing iSNV, data from only those participants were included for whom sequence data from baseline and at least one follow-up time point were available. iSNV analysis was performed using PASeq SARS-CoV-2 pipeline (www.paseq.org). Briefly, raw sequence files were quality filtered and adapter-trimmed using trimmomatic (v0.30). Contaminating sequences were filtered out using BBMap Suite (v35.76). Duplicated reads were detected using fastuniq (v1.1). High-quality nonredundant reads were then aligned to SARS-CoV-2 Wuhan reference (NC_045512.2) using Bowtie2 (v.2.3.2). Resulting alignments were processed with samtools (v.1.2) and iVar (v1.4.2) to obtain nucleotide variant VCF files. Nucleotide variants present at 100% frequency of the total viral population at all time points indicative of lineage-defining mutations were excluded from the iSNV analysis. Genetic diversity between multiple sequences of an individual was assessed by average pairwise distance in MEGA at both nucleotide and amino acid levels using the consensus *S* gene sequence. mAb escape mutations were defined per Emergency Use Authorization factsheet for each mAbs as listed in table S5 (*53*–*57*).

Generalized estimating equation

GEE was performed using "geepack" package (version 1.3.9) in R (*58*). In the GEE model, family was set as "gaussian," and the correlation structure ("corstr") was set as "independence." Quasi Information Criterion (QIC) was used to compare models using "independence," "exchangeable," and "ar1," and the one with "independence" had the lowest QIC. mAb use, weeks since symptom onset or first positive PCR test or antigen test, numbers of vaccinations before enrollment, sex, and age were adjusted for in these models. Logarithm base 10 of the nAb titers were treated as dependent variables and other variables as independent. Coefficients for all the independent variables were then transformed to the power of 10 and are shown in fig. S3 as fold change compared to reference group.

Propensity score matching for delayed versus early viral RNA clearance

We defined delayed viral RNA clearance as clearance of SARS-CoV-2 viral RNA beyond day 30 or positive viral RNA beyond day 10 and then lost to follow-up. To compare the T cell responses while controlling for humoral immunity, we matched participants with delayed viral clearance ($n = 5$) in a 1:3 ratio to those with early clearance. Because nucleocapsid binding Ab titers were not affected by mAb use, we chose to use nucleocapsid binding Ab as a marker for endogenous humoral responses. Participant ID 245 only had nucleocapsid-specific antibodies at blood draw 2, and the value was below or equal to the quantification range of 0.11 IU/ml; thus, we input binding Ab titers at blood draw 1 with the same titers of binding Ab at blood draw 2, only for propensity matching purposes. "MatchIt" package was used (version 4.5.5) to perform the propensity matching (*59*) using default parameters except method = "optimal."

Statistical analysis

All raw, individual-level data for experiments where $n < 20$ are presented in data file S1. Categorical variables were summarized using total number and percentage, and we used either chi-square test or Fisher's exact test when chi-square test goodness-of-fit rule was not met to determine significance. Continuous variables were summarized with median and interquartile ranges and compared with nonparametric methods to determine significance: Wilcoxon rank-sum test was used to compare two groups, and Dunn's test with Benjamini-Hochberg adjustment was used to compare three or more groups. Within group comparisons were conducted using paired Wilcoxon signed-rank test without adjustment for multiple comparisons to determine significance. We also used GEE with Gaussian estimation to evaluate between-group differences accounting for repeated measurement during longitudinal follow-up. We did not use parametric methods to evaluate continuous variables, and thus, we allowed non-normal distributed data. Proportional hazards assumption was not met for Cox regression models, and thus we also used RMST model to validate our findings (survRM2 package in R version 1.0.4). Two-tailed tests were used for all the analyses, and $P < 0.05$ was considered statistically significant unless specified otherwise. Data presented in this study represented biological replicates. R (4.3.0) was used for statistical analyses.

Supplementary Materials

This PDF file includes:

Fig. S1 to S6
Tables S1 to S5

Other Supplementary Material for this manuscript includes the following:

Data file S1
MDAR Reproducibility Checklist

REFERENCES AND NOTES

1. H. M. El Sahly, L. R. Baden, B. Essink, S. Doblecki-Lewis, J. M. Martin, E. J. Anderson, T. B. Campbell, J. Clark, L. A. Jackson, C. J. Fichtenbaum, M. Zervos, B. Rankin, F. Eder, G. Feldman, C. Kennelly, L. Han-Conrad, M. Levin, K. M. Neuzil, L. Corey, P. Gilbert, H. Janes, D. Follmann, M. Marovich, L. Polakowski, J. R. Mascola, J. E. Ledgerwood, B. S. Graham, A. August, H. Clouting, W. Deng, S. Han, B. Leav, D. Manzo, R. Pajon, F. Schödel, J. E. Tomassini, H. Zhou, J. Miller, COVE Study Group, Efficacy of the mRNA-1273 SARS-CoV-2 Vaccine at Completion of Blinded Phase. *N. Engl. J. Med.* **385**, 1774–1785 (2021).
2. E. D. Moreira Jr., N. Kitchin, X. Xu, S. S. Dychter, S. Lockhart, A. Gurtman, J. L. Perez, C. Zerbini, M. E. Dever, T. W. Jennings, D. M. Brandon, K. D. Cannon, M. J. Koren, D. S. Denham, M. Berhe, D. Fitz-Patrick, L. L. Hammitt, N. P. Klein, H. Nell, G. Keep, X. Wang, K. Koury, K. A. Swanson, D. Cooper, C. Lu, Ö. Türeci, E. Lagkadinou, D. B. Tresnan, P. R. Dormitzer, U. Şahin, W. C. Gruber, K. U. Jansen, Safety and efficacy of a third dose of BNT162b2 COVID-19 vaccine. *N. Engl. J. Med.* **386**, 1910–1921 (2022).
3. O. J. Watson, G. Barnsley, J. Toor, A. B. Hogan, P. Winskill, A. C. Ghani, Global impact of the first year of COVID-19 vaccination: A mathematical modelling study. *Lancet Infect. Dis.* **22**, 1293–1302 (2022).
4. G. Haidar, M. Agha, A. Bilderback, A. Lukanski, K. Linstrum, R. Troyan, S. Rothenberger, D. K. McMahon, M. D. Crandall, M. D. Sobolewksi, P. N. Enick, J. L. Jacobs, K. Collins, C. Klamar-Blain, B. J. C. Macatangay, U. M. Parikh, A. Heaps, L. Coughenour, M. B. Schwartz, J. M. Dueker, F. P. Silveira, M. E. Keebler, A. Humar, J. D. Luketich, M. R. Morrell, J. M. Pilewski, J. F. McDyer, B. Pappu, R. L. Ferris, S. M. Marks, J. Mahon, K. Mulvey, S. Hariharan, G. M. Updike, L. Brock, R. Edwards, R. H. Beigi, P. L. Kip, A. Wells, T. Minnier, D. C. Angus, J. W. Mellors, Prospective evaluation of coronavirus disease 2019 (COVID-19) vaccine responses across a broad spectrum of immunocompromising conditions: The COVID-19 Vaccination in the Immunocompromised Study (COVICS). *Clin. Infect. Dis.* **75**, e630–e644 (2022).
5. L. Wieske, K. P. J. van Dam, M. Steenhuis, E. W. Stalman, L. Y. L. Kummer, Z. L. E. van Kempen, J. Killestein, A. G. Volkers, S. W. Tas, L. Boekel, G. J. Wolbink, A. J. van der Kooi, J. Raaphorst, M. Löwenberg, R. B. Takkenberg, G. D'Haens, P. I. Spuls, M. W. Bekkenk, A. H. Musters, N. F. Post, A. L. Bosma, M. L. Hilhorst, Y. Vegting, F. J. Bemelman, A. E. Voskuyl, B. Broens, A. P. Sanchez, C. van Els, J. de Wit, A. Rutgers, K. de Leeuw, B. Horváth, J. Verschuuren, A. M. Ruiter, L. van Ouwerkerk, D. van der Woude, R. C. F. Allaart, Y. K. O. Teng, P. van Paassen, M. H. Busch, P. B. P. Jallah, E. Brusse, P. A. van Doorn, A. E. Baars, D. J. Hijnen, C. R. G. Schreurs, W. L. van der Pol, H. S. Goedee, S. Keijzer, J. B. D. Keijser, A. Boogaard, O. Cristianawati, A. Ten Brinke, N. J. M. Verstegen, K. A. H. Zwinderman, S. M. van Ham, T. W. Kuijpers, T. Rispens, F. Eftimov, T2B! Immunity against SARS-CoV-2 study group, Humoral responses after second and third SARS-CoV-2 vaccination in patients with immune-mediated inflammatory disorders on immunosuppressants: A cohort study. *Lancet Rheumatol.* **4**, e338–e350 (2022).

6. J. D. Kelly, S. Leonard, K. J. Hoggatt, W. J. Boscardin, E. N. Lum, T. A. Moss-Vazquez, R. Andino, J. K. Wong, A. Byers, D. M. Bravata, P. C. Tien, S. Keyhani, Incidence of Severe COVID-19 illness following vaccination and booster with BNT162b2, mRNA-1273, and Ad26.COV2.S vaccines. *JAMA* **328**, 1427–1437 (2022).
7. U. Agrawal, S. Bedston, C. McCowan, J. Oke, L. Patterson, C. Robertson, A. Akbari, A. Azcoaga-Lorenzo, D. T. Bradley, A. F. Fagbamigbe, Z. Grange, E. C. R. Hall, M. Joy, S. V. Katikireddi, S. Kerr, L. Ritchie, S. Murphy, R. K. Owen, I. Rudan, S. A. Shah, C. R. Simpson, F. Torabi, R. S. M. Tsang, S. de Lusignan, R. A. Lyons, D. O'Reilly, A. Sheikh, Severe COVID-19 outcomes after full vaccination of primary schedule and initial boosters: Pooled analysis of national prospective cohort studies of 30 million individuals in England, Northern Ireland, Scotland, and Wales. *Lancet* **400**, 1305–1320 (2022).
8. D. Planas, D. Veyer, A. Baidaliuk, I. Staropoli, F. Guivel-Benhassine, M. M. Rajah, C. Planchais, F. Porrot, N. Robillard, J. Puech, M. Prot, F. Gallais, P. Gantner, A. Velay, J. Le Guen, N. Kassis-Chikhani, D. Edriss, L. Belec, A. Seve, L. Courtellemont, H. Péré, L. Hocqueloux, S. Fafi-Kremer, T. Prazuck, H. Mouquet, T. Bruel, E. Simon-Lorière, F. A. Rey, O. Schwartz, Reduced sensitivity of SARS-CoV-2 variant Delta to antibody neutralization. *Nature* **596**, 276–280 (2021).
9. M. Hoffmann, H. Hofmann-Winkler, N. Krüger, A. Kempf, I. Nehlmeier, L. Graichen, P. Arora, A. Sidarovich, A.-S. Moldenhauer, M. S. Winkler, S. Schulz, H.-M. Jäck, M. V. Stankov, G. M. N. Behrens, S. Pöhlmann, SARS-CoV-2 variant B.1.617 is resistant to bamlanivimab and evades antibodies induced by infection and vaccination. *Cell Rep.* **36**, 109415 (2021).
10. Q. Wang, Y. Guo, S. Iketani, M. S. Nair, Z. Li, H. Mohri, M. Wang, J. Yu, A. D. Bowen, J. Y. Chang, J. G. Shah, N. Nguyen, Z. Chen, K. Meyers, M. T. Yin, M. E. Sobieszczyk, Z. Sheng, Y. Huang, L. Liu, D. D. Ho, Antibody evasion by SARS-CoV-2 Omicron subvariants BA.2.12.1, BA.4 and BA.5. *Nature* **608**, 603–608 (2022).
11. S. Weigang, J. Fuchs, G. Zimmer, D. Schnepf, L. Kern, J. Beer, H. Luxenburger, J. Ankerhold, V. Falcone, J. Kemming, M. Hofmann, R. Thimme, C. Neumann-Haefelin, S. Ulferts, R. Grosse, D. Hornuss, Y. Tanriver, S. Rieg, D. Wagner, D. Huzly, M. Schwemmle, M. Panning, G. Kochs, Within-host evolution of SARS-CoV-2 in an immunosuppressed COVID-19 patient as a source of immune escape variants. *Nat. Commun.* **12**, 6405 (2021).
12. S. Cele, F. Karim, G. Lustig, J. E. San, T. Hermanus, H. Tegally, J. Snyman, T. Moyo-Gwete, E. Wilkinson, M. Bernstein, K. Khan, S. H. Hwa, S. W. Tilles, L. Singh, J. Giandhari, N. Mthabela, M. Mazibuko, Y. Ganga, B. I. Gosnell, S. S. A. Karim, W. Hanekom, W. C. Van Voorhis, T. Ndung'u, C.-K. Team, R. J. Lessells, P. L. Moore, M. S. Moosa, T. de Oliveira, A. Sigal, SARS-CoV-2 prolonged infection during advanced HIV disease evolves extensive immune escape. *Cell Host Microbe* **30**, 154–162.e5 (2022).
13. B. Choi, M. C. Choudhary, J. Regan, J. A. Sparks, R. F. Padera, X. Qiu, I. H. Solomon, H.-H. Kuo, J. Boucau, K. Bowman, U. D. Adhikari, M. L. Winkler, A. A. Mueller, T. Y. T. Hsu, M. Desjardins, L. R. Baden, B. T. Chan, B. D. Walker, M. Lichterfeld, M. Brigl, D. S. Kwon, S. Kanjilal, E. T. Richardson, A. H. Jonsson, G. Alter, A. K. Barczak, W. P. Hanage, X. G. Yu, G. D. Gaiha, M. S. Seaman, M. Cernadas, J. Z. Li, Persistence and evolution of SARS-CoV-2 in an immunocompromised host. *N. Engl. J. Med.* **383**, 2291–2293 (2020).
14. M. K. Hensley, W. G. Bain, J. Jacobs, S. Nambulli, U. Parikh, A. Cillo, B. Staines, A. Heaps, M. D. Sobolewski, L. J. Rennick, B. J. C. Macatangay, C. Klamar-Blain, G. D. Kitsios, B. Methé, A. Somasundaram, T. C. Bruno, C. Cardello, F. Shan, C. Workman, P. Ray, A. Ray, J. Lee, R. Sethi, W. E. Schwarzmann, M. S. Ladinsky, P. J. Bjorkman, D. A. Vignali, W. P. Duprex, M. E. Agha, J. W. Mellors, K. D. McCormick, A. Morris, G. Haidar, Intractable coronavirus disease 2019 (COVID-19) and prolonged severe acute respiratory syndrome coronavirus 2 (SARS-CoV-2) replication in a chimeric antigen receptor-modified t-cell therapy recipient: A case study. *Clin. Infect. Dis.* **73**, e815–e821 (2021).
15. S. Harari, M. Tahor, N. Rutsinsky, S. Meijer, D. Miller, O. Henig, O. Halutz, K. Levytskyi, R. Ben-Ami, A. Adler, Y. Paran, A. Stern, Drivers of adaptive evolution during chronic SARS-CoV-2 infections. *Nat. Med.* **28**, 1501–1508 (2022).
16. M. C. Choudhary, C. R. Crain, X. Qiu, W. Hanage, J. Z. Li, Severe acute respiratory syndrome coronavirus 2 (SARS-CoV-2) sequence characteristics of coronavirus disease 2019 (COVID-19) persistence and reinfection. *Clin. Infect. Dis.* **74**, 237–245 (2022).
17. J. Boucau, C. Marino, J. Regan, R. Uddin, M. C. Choudhary, J. P. Flynn, G. Chen, A. M. Stuckwisch, J. Mathews, M. Y. Liew, A. Singh, T. Lipiner, A. Kittilson, M. Melberg, Y. Li, R. F. Gilbert, Z. Reynolds, S. L. Iyer, G. C. Chamberlin, T. D. Vyas, M. B. Goldberg, J. M. Vyas, J. Z. Li, J. E. Lemieux, M. J. Siedner, A. K. Barczak, Duration of shedding of culturable virus in SARS-CoV-2 Omicron (BA.1) Infection. *N. Engl. J. Med.* **387**, 275–277 (2022).
18. M. S. Seaman, M. J. Siedner, J. Boucau, C. L. Lavine, F. Ghantous, M. Y. Liew, J. I. Mathews, A. Singh, C. Marino, J. Regan, R. Uddin, M. C. Choudhary, J. P. Flynn, G. Chen, A. M. Stuckwisch, T. Lipiner, A. Kittilson, M. Melberg, R. F. Gilbert, Z. Reynolds, S. L. Iyer, G. C. Chamberlin, T. D. Vyas, J. M. Vyas, M. B. Goldberg, J. Luban, J. Z. Li, A. K. Barczak, J. E. Lemieux, Vaccine breakthrough infection leads to distinct profiles of neutralizing antibody responses by SARS-CoV-2 variant. *JCI Insight* **7**, e159944 (2022).
19. M. J. Siedner, J. Boucau, R. F. Gilbert, R. Uddin, J. Luu, S. Haneuse, T. Vyas, Z. Reynolds, S. Iyer, G. C. Chamberlin, R. H. Goldstein, C. M. North, C. A. Sacks, J. Regan, J. P. Flynn, M. C. Choudhary, J. M. Vyas, A. K. Barczak, J. E. Lemieux, J. Z. Li, Duration of viral shedding and culture positivity with postvaccination SARS-CoV-2 delta variant infections. *JCI Insight* **7**, e155483 (2022).
20. V. A. Avanzato, M. J. Matson, S. N. Seifert, R. Pryce, B. N. Williamson, S. L. Anzick, K. Barbian, S. D. Judson, E. R. Fischer, C. Martens, T. A. Bowden, E. de Wit, F. X. Riedo, V. J. Munster, Case study: Prolonged infectious SARS-CoV-2 shedding from an asymptomatic immunocompromised individual with cancer. *Cell* **183**, 1901–1912.e9 (2020).
21. C. Chaguza, A. M. Hahn, M. E. Petrone, S. Zhou, D. Ferguson, M. I. Breban, K. Pham, M. A. Peña-Hernández, C. Castaldi, V. Hill, W. Schulz, R. I. Swanstrom, S. C. Roberts, N. D. Grubaugh, Accelerated SARS-CoV-2 intrahost evolution leading to distinct genotypes during chronic infection. *Cell Rep. Med.* **4**, 100943 (2023).
22. B. Bailly, H. Péré, D. Veyer, A. Berceanu, E. Daguindau, P. Roux, O. Hermine, X. de Lamballerie, P. Bastard, K. Lacombe, B. Autran, F. A. Delettre, J. L. Casanova, S. Imbeaud, A. L. Clairet, M. Kroemer, L. Spehner, N. Robillard, J. Puech, S. Marty-Quinternet, Q. Lepiller, C. Chirouze, K. Bouiller, Persistent coronavirus disease 2019 (COVID-19) in an immunocompromised host treated by severe acute respiratory syndrome coronavirus 2 (SARS-CoV-2)-specific monoclonal antibodies. *Clin. Infect. Dis.* **74**, 1706–1707 (2022).
23. A. Truffot, J. Andréani, M. Le Maréchal, A. Caporossi, O. Epaulard, R. Germi, P. Poignard, S. Larrat, SARS-CoV-2 variants in immunocompromised patient given antibody monotherapy. *Emerg. Infect. Dis.* **27**, 2725–2728 (2021).
24. A. Gupta, A. Konnova, M. Smet, M. Berkell, A. Savoldi, M. Morra, V. Van Averbeke, F. H. De Winter, D. Peserico, E. Danese, A. Hotterbeekx, E. Righi, mAb ORCHESTRA working group; Pasquale De Nardo, P. De Nardo, E. Tacconelli, S. Malhotra-Kumar, S. Kumar-Singh, Host immunological responses facilitate development of SARS-CoV-2 mutations in patients receiving monoclonal antibody treatments. *J. Clin. Invest.* **133**, e166032 (2023).
25. J. H. Baang, C. Smith, C. Mirabelli, A. L. Valesano, D. M. Manthei, M. A. Bachman, C. E. Wobus, M. Adams, L. Washer, E. T. Martin, A. S. Lauring, Prolonged severe acute respiratory syndrome coronavirus 2 replication in an immunocompromised patient. *J Infect Dis* **223**, 23–27 (2021).
26. Y. Bronstein, A. Adler, H. Katash, O. Halutz, Y. Herishanu, K. Levytskyi, Evolution of spike mutations following antibody treatment in two immunocompromised patients with persistent COVID-19 infection. *J. Med. Virol.* **94**, 1241–1245 (2022).
27. A. S. Gonzalez-Reiche, H. Alshammary, S. Schaefer, G. Patel, J. Polanco, J. M. Carreno, A. A. Amoako, A. Rooker, C. Cognigni, D. Floda, A. van de Guchte, Z. Khalil, K. Farrugia, N. Assad, J. Zhang, B. Alburquerque, PARIS/PSP study group; Levy A Sominsky, C. Gleason, K. Srivastava, R. Sebra, J. D. Ramirez, R. Banu, P. Shrestha, F. Krammer, A. Paniz-Mondolfi, E. M. Sordillo, V. Simon, H. van Bakel, Sequential intrahost evolution and onward transmission of SARS-CoV-2 variants. *Nat. Commun.* **14**, 3235 (2023).
28. M. C. Choudhary, K. W. Chew, R. Deo, J. P. Flynn, J. Regan, C. R. Crain, C. Moser, M. D. Hughes, J. Ritz, R. M. Ribeiro, R. Ke, J. A. Dragavon, A. C. Javan, A. Nirula, P. Klekotka, A. L. Greninger, C. V. Fletcher, E. S. Daar, D. A. Wohl, J. J. Eron, J. S. Currier, U. M. Parikh, S. F. Sieg, A. S. Perelson, R. W. Coombs, D. M. Smith, J. Z. Li, Emergence of SARS-CoV-2 escape mutations during Bamlanivimab therapy in a phase II randomized clinical trial. *Nat. Microbiol.* **7**, 1906–1917 (2022).
29. S. A. Kemp, D. A. Collier, R. P. Datir, I. Ferreira, S. Gayed, A. Jahun, M. Hosmillo, C. Rees-Spear, P. Mlcochova, I. U. Lumb, D. J. Roberts, A. Chandra, N. Temperton, K. Sharrocks, E. Blane, Y. Modis, K. E. Leigh, J. A. G. Briggs, M. J. van Gils, K. G. C. Smith, J. R. Bradley, C. Smith, R. Doffinger, L. Ceron-Gutierrez, G. Barcenas-Morales, D. D. Pollock, R. A. Goldstein, A. Smielewska, J. P. Skittrall, T. Gouliouris, I. G. Goodfellow, E. Gkrania-Klotsas, C. J. R. Illingworth, L. E. McCoy, R. K. Gupta, SARS-CoV-2 evolution during treatment of chronic infection. *Nature* **592**, 277–282 (2021).
30. S. A. Apostolidis, M. Kakara, M. M. Painter, R. R. Goel, D. Mathew, K. Lenzi, A. Rezk, K. R. Patterson, D. A. Espinoza, J. C. Kadri, D. M. Markowitz, C. E. Markowitz, I. Mexhitaj, D. Jacobs, A. Babb, M. R. Betts, E. T. L. Prak, D. Weiskopf, A. Grifoni, K. A. Lundgreen, S. Gouma, A. Sette, P. Bates, S. E. Hensley, A. R. Greenplate, E. J. Wherry, R. Li, A. Bar-Or, Cellular and humoral immune responses following SARS-CoV-2 mRNA vaccination in patients with multiple sclerosis on anti-CD20 therapy. *Nat. Med.* **27**, 1990–2001 (2021).
31. R. Zonozi, L. C. Walters, A. Shulkin, V. Naranbhai, P. Nithagon, G. Sauvage, C. Kaeske, K. Cosgrove, A. Nathan, R. Tano-Menka, A. C. Gayton, M. A. Getz, F. Senjobe, D. Worrall, A. J. Iafrate, C. Fromson, S. B. Montesi, D. A. Rao, J. A. Sparks, Z. S. Wallace, J. R. Farmer, B. D. Walker, R. C. Charles, K. Laliberte, J. L. Niles, G. D. Gaiha, T cell responses to SARS-CoV-2 infection and vaccination are elevated in B cell deficiency and reduce risk of severe COVID-19. *Sci. Transl. Med.* **15**, eadh4529 (2023).
32. V. Dioverti, S. Salto-Alejandre, G. Haidar, Immunocompromised patients with protracted COVID-19: A review of "long persisters". *Curr. Transplant. Rep.* **9**, 209–218 (2022).
33. V. Nussenblatt, A. E. Roder, S. Das, E. de Wit, J. H. Youn, S. Banakis, A. Mushegian, C. Mederos, W. Wang, M. Chung, L. Pérez-Pérez, T. Palmore, J. N. Brudno, J. N. Kochenderfer, E. Ghedin, Yearlong COVID-19 infection reveals within-host evolution of SARS-CoV-2 in a patient with B-cell depletion. *J Infect Dis* **225**, 1118–1123 (2022).
34. T. Aydillo, A. S. Gonzalez-Reiche, S. Aslam, A. van de Guchte, Z. Khan, A. Obla, J. Dutta, H. van Bakel, J. Aberg, A. García-Sastre, G. Shah, T. Hohl, G. Papanicolaou, M. A. Perales, K. Sepkowitz, N. E. Babady, M. Kamboj, Shedding of viable SARS-CoV-2 after immunosuppressive therapy for cancer. *N. Engl. J. Med.* **383**, 2586–2588 (2020).

35. S. Gandhi, J. Klein, A. J. Robertson, M. A. Peña-Hernández, M. J. Lin, P. Roychoudhury, P. Lu, J. Fournier, D. Ferguson, S. A. K. Mohamed Bakhash, M. Catherine Muenker, A. Srivathsan, E. A. Wunder Jr., N. Kerantzas, W. Wang, B. Lindenbach, A. Pyle, C. B. Wilen, O. Ogbuagu, A. L. Greninger, A. Iwasaki, W. L. Schulz, A. I. Ko, De novo emergence of a remdesivir resistance mutation during treatment of persistent SARS-CoV-2 infection in an immunocompromised patient: A case report. *Nat. Commun.* **13**, 1547 (2022).
36. C. L. Gordon, O. C. Smibert, N. E. Holmes, K. Y. L. Chua, M. Rose, G. Drewett, F. James, E. Mouhtouris, T. H. O. Nguyen, W. Zhang, L. Kedzierski, L. C. Rowntree, B. Y. Chua, L. Caly, M. G. Catton, J. Druce, M. Sait, T. Seemann, N. L. Sherry, B. P. Howden, K. Kedzierska, J. C. Kwong, J. A. Trubiano, Defective severe acute respiratory syndrome coronavirus 2 immune responses in an immunocompromised individual with prolonged viral replication. *Open Forum Infect. Dis.* **8**, ofab359 (2021).
37. I. Monrad, S. R. Sahlertz, S. S. F. Nielsen, L. Pedersen, M. S. Petersen, C. M. Kobel, I. H. Tarpgaard, M. Storgaard, K. L. Mortensen, M. H. Schleimann, M. Tolstrup, L. K. Vibholm, Persistent severe acute respiratory syndrome coronavirus 2 infection in immunocompromised host displaying treatment induced viral evolution. *Open Forum Infect. Dis.* **8**, ofab295 (2021).
38. K. M. Braun, G. K. Moreno, C. Wagner, M. A. Accola, W. M. Rehrauer, D. A. Baker, K. Koelle, D. H. O'Connor, T. Bedford, T. C. Friedrich, L. H. Moncla, Acute SARS-CoV-2 infections harbor limited within-host diversity and transmit via tight transmission bottlenecks. *PLOS Pathog.* **17**, e1009849 (2021).
39. K. K. K. Ko, H. Yingtaweesittikul, T. T. Tan, L. Wijaya, D. Y. Cao, S. S. Goh, N. B. Abdul Rahman, K. X. L. Chan, H. M. Tay, J. H. C. Sim, K. S. Chan, L. L. E. Oon, N. Nagarajan, C. Suphavilai, Emergence of SARS-CoV-2 spike mutations during prolonged infection in immunocompromised hosts. *Microbiol. Spectr.* **10**, e0079122 (2022).
40. K. A. Lythgoe, M. Hall, L. Ferretti, M. de Cesare, G. MacIntyre-Cockett, A. Trebes, M. Andersson, N. Otecko, E. L. Wise, N. Moore, J. Lynch, S. Kidd, N. Cortes, M. Mori, R. Williams, G. Vernet, A. Justice, A. Green, S. M. Nicholls, M. A. Ansari, L. Abeler-Dörner, C. E. Moore, T. E. A. Peto, D. W. Eyre, R. Shaw, P. Simmonds, D. Buck, J. A. Todd, T. R. Connor, S. Ashraf, A. da Silva Filipe, J. Shepherd, E. C. Thomson, D. Bonsall, C. Fraser, T. Golubchik, SARS-CoV-2 within-host diversity and transmission. *Science* **372**, eabg0821 (2021).
41. A. L. Valesano, K. E. Rumfelt, D. E. Dimcheff, C. N. Blair, W. J. Fitzsimmons, J. G. Petrie, E. T. Martin, A. S. Lauring, Temporal dynamics of SARS-CoV-2 mutation accumulation within and across infected hosts. *PLOS Pathog.* **17**, e1009499 (2021).
42. A. Soresina, D. Moratto, M. Chiarini, C. Paolillo, G. Baresi, E. Focà, M. Bezzi, B. Baronio, M. Giacomelli, R. Badolato, Two X-linked agammaglobulinemia patients develop pneumonia as COVID-19 manifestation but recover. *Pediatr. Allergy Immunol.* **31**, 565–569 (2020).
43. T. Dangi, S. Sanchez, J. Class, M. C. Richner, L. Visvabharathy, Y. R. Chung, K. Bentley, R. J. Stanton, I. J. Koralnik, J. M. Richner, P. Penaloza-MacMaster, Improved control of SARS-CoV-2 by treatment with nucleocapsid-specific monoclonal antibody. *J. Clin. Invest.* **132**, e162282 (2022).
44. R. Kundu, J. S. Narean, L. Wang, J. Fenn, T. Pillay, N. D. Fernandez, E. Conibear, A. Koycheva, M. Davies, M. Tolosa-Wright, S. Hakki, R. Varro, E. McDermott, S. Hammett, J. Cutajar, R. S. Thwaites, E. Parker, C. Rosadas, M. McClure, R. Tedder, G. P. Taylor, J. Dunning, A. Lalvani, Cross-reactive memory T cells associate with protection against SARS-CoV-2 infection in COVID-19 contacts. *Nat. Commun.* **13**, 80 (2022).
45. K. Maneikis, K. Šablauskas, U. Ringelevičiūtė, V. Vaitekėnaitė, R. Čekauskienė, L. Kryžauskaitė, D. Naumovas, V. Banys, V. Pečeliūnas, T. Beinortas, L. Griškevičius, Immunogenicity of the BNT162b2 COVID-19 mRNA vaccine and early clinical outcomes in patients with haematological malignancies in Lithuania: a national prospective cohort study. *Lancet Haematol.* **8**, e583–e592 (2021).
46. J. Fajnzylber, J. Regan, K. Coxen, H. Corry, C. Wong, A. Rosenthal, D. Worrall, F. Giguel, A. Piechocka-Trocha, C. Atyeo, S. Fischinger, A. Chan, K. T. Flaherty, K. Hall, M. Dougan, E. T. Ryan, E. Gillespie, R. Chishti, Y. Li, N. Jilg, D. Hanidziar, R. M. Baron, L. Baden, A. M. Tsibris, K. A. Armstrong, D. R. Kuritzkes, G. Alter, B. D. Walker, X. Yu, J. Z. Li, Massachusetts Consortium for Pathogen Readiness, SARS-CoV-2 viral load is associated with increased disease severity and mortality. *Nat. Commun.* **11**, 5493 (2020).
47. R. Deo, M. C. Choudhary, C. Moser, J. Ritz, E. S. Daar, D. A. Wohl, A. L. Greninger, J. J. Eron, J. S. Currier, M. D. Hughes, D. M. Smith, K. W. Chew, J. Z. Li, ACTIV-/A Study Team, Symptom and viral rebound in untreated SARS-CoV-2 infection. *Ann. Intern. Med.* **176**, 348–354 (2023).
48. A. Nathan, E. J. Rossin, C. Kaseke, R. J. Park, A. Khatri, D. Koundakjian, J. M. Urbach, N. K. Singh, A. Bashirova, R. Tano-Menka, F. Senjobe, M. T. Waring, A. Piechocka-Trocha, W. F. Garcia-Beltran, A. J. Iafrate, V. Naranbhai, M. Carrington, B. D. Walker, G. D. Gaiha, Structure-guided T cell vaccine design for SARS-CoV-2 variants and sarbecoviruses. *Cell* **184**, 4401–4413.e10 (2021).
49. P. L. Tzou, K. Tao, S. L. K. Pond, R. W. Shafer, Coronavirus Resistance Database (CoV-RDB): SARS-CoV-2 susceptibility to monoclonal antibodies, convalescent plasma, and plasma from vaccinated persons. *PLOS ONE* **17**, e0261045 (2022).
50. P. L. Tzou, K. Tao, M. K. Sahoo, S. L. Kosakovsky Pond, B. A. Pinsky, R. W. Shafer, Sierra SARS-CoV-2 sequence and antiviral resistance analysis program. *J. Clin. Virol.* **157**, 105323 (2022).
51. J. Z. Li, N. Stella, M. C. Choudhary, A. Javed, K. Rodriguez, H. Ribaudo, M. Y. Moosa, J. Brijkumar, S. Pillay, H. Sunpath, M. Noguera-Julian, R. Paredes, B. Johnson, A. Edwards, V. C. Marconi, D. R. Kuritzkes, Impact of pre-existing drug resistance on risk of virological failure in South Africa. *J. Antimicrob. Chemother.* **76**, 1558–1563 (2021).
52. I. Aksamentov, C. Roemer, E. B. Hodcroft, R. A. Neher, Nextclade: clade assignment, mutation calling and quality control for viral genomes. *J. Open Source Softw.* **6**, 3773 (2021).
53. FDA, Fact sheet for healthcare providers: Emergency use authorization for Sotrovimab (FDA, 2023).
54. FDA, Fact sheet for health care providers: Emergency use authorization (EUA) of REGEN-COV (Casirivimab and Imdevimab) (FDA, 2022).
55. FDA, Fact sheet for healthcare providers: Emergency use authorization for Bebtelovimab (FDA, 2022).
56. FDA, Fact sheet for health care providers: Emergency use authorization (EUA) of Bamlanivimab And Etesevimab (2022)
57. FDA, Fact sheet for healthcare providers: Emergency use authorization for Evusheld (Tixagevimab co-packaged with Cilgavimab) (FDA, 2023).
58. S. Højsgaard, U. Halekoh, J. Yan, The R Package geepack for Generalized Estimating Equations. *J. Stat. Softw.* **15**, 1–11 (2005).
59. D. Ho, K. Imai, G. King, E. A. Stuart, MatchIt: Nonparametric preprocessing for parametric causal inference. *J. Stat. Softw.* **42**, 1–28 (2011).

Acknowledgments: We thank all the participants for their participation in this important study. We thank all the health care workers who take care of them and refer them to the POSITIVES study. **Funding:** This work was supported by the National Institutes of Health (grants U19 AI110818 and R01 AI176287), the Massachusetts Consortium for Pathogen Readiness SARS-CoV-2 Variants Program (MassCPR), and the Massachusetts General Hospital Department of Medicine. J.A.S. and Z.S.W. are supported by the National Institute of Arthritis and Musculoskeletal and Skin Diseases (grant R01 AR080659). J.A.S. is also supported by the Llura Gund Award funded by the Gordon and Llura Gund Foundation. G.D.G. is supported by the NIH (grants DP2AI154421, R01AI176533, and DP1DA058476), the Bill and Melinda Gates Foundation, a Burroughs Wellcome Career Award for Medical Scientists, and a Howard Goodman Fellowship. J.Z.L. is also supported by a grant from the Investigator-Initiated Studies Program of Merck Sharp & Dohme LLC. The opinions expressed in this paper are those of the authors and do not necessarily reflect those of Merck Sharp & Dohme LLC. Y.L. was supported by Rustbelt CFAR (Case Western Reserve University/University Hospitals Cleveland Medical Center and University of Pittsburgh, P30 AI036219). The BSL3 laboratory where viral culture work was performed is supported by the Harvard CFAR (P30 AI060354). The funders had no role in the study design; in the collection, analysis, and interpretation of data; in the writing of the manuscript; or in the decision to submit the manuscript for publication. **Authors contributions:** M.J.S., A.K.B., J.E.L., J.Z.L. conceptualized the study. J.R., J.B., G.E.E., C.M., and J.P.F. conducted the virology assays. M.C.C., R.U., R.D., J.E.L., and J.Z.L. conducted the sequence analyses. T.S., M.S.S., and M.Y.L. conducted the Ab assays. A.N., M.A.G., and G.D.G. performed the T cell assays. Z.R., M.B., R.F.G., D.T., S.S., T.D.V., S.P.H., L.A.N., B.C., M.C., Z.S.W., and J.A.S. J.M.V. coordinated the study enrollment, referral, follow-up, or sample collection. Y.L., Y.K., Z.S.W., and J.A.S. performed chart review. Y.L., M.C.C., J.R., and R.D. performed analysis. M.J.S. and R.F.G. managed the database. Y.L., M.C.C., J.R., and J.Z.L. wrote the first draft. All authors reviewed the manuscript. **Competing interests:** S.P.H. receives research funding from GSK and have served as an advisor to Pfizer. J.Z.L. is supported by a grant from the Investigator-Initiated Studies Program of Merck Sharp & Dohme LLC. The opinions expressed in this paper are those of the authors and do not necessarily reflect those of Merck Sharp & Dohme LLC. Y.L. is a topic editor for DynaMed. All other authors declare that they have no competing interests. **Data and materials availability:** All data associated with this study are present in the paper or the supplementary materials. Next-generation sequencing data SRA accession number is PRJNA1027562.

Submitted 5 August 2023
Accepted 18 December 2023
Published 24 January 2024
10.1126/scitranslmed.adk1599